JOURNAL OF AGRICULTURAL AND FOOD CHEMISTRY

Alginate and Chitosan Functionalization for Micronutrient Encapsulation

JAEJOON HAN, ANNE-SOPHIE GUENIER, STÉPHANE SALMIERI, AND MONIQUE LACROIX*

Institut National de la Recherche Scientifique, Institut Armand-Frappier, 531 Boulevard des Prairies, Laval, Québec H7V 1B7, Canada

A new method for encapsulation of micronutrients was successfully developed. The encapsulation matrix consisted of two polymers (alginate and chitosan), which were functionalized by acylation with palmitoyl chloride. The structural modifications of polymers were confirmed by Fourier transform infrared (FTIR) spectroscopy. Beads were formed by ionic gelation, and their mechanical and physical characteristics (puncture strength and deformation, viscoelasticity, water vapor permeability, and rate of gel swelling) were evaluated using beads or films made of bead-forming solutions. Functionalization increased elasticity and water impermeability of polymer films. Stability of selected encapsulated micronutrients (ferrous fumarate, ascorbic acid, and β-carotene) was also evaluated under two levels of temperature (23 and 45 °C) and relative humidity (56 and 100%) for 6 months. Encapsulation strongly increased the stability of micronutrients. No difference was observed in the encapsulated micronutrients' stability between nonfunctionalized and functionalized beads. Finally, a release study in gastrointestinal media was conducted. Results showed that beads were not susceptible to enzymatic and acidic attacks during stomach transit. This research demonstrates the potential of a new encapsulation method to protect bioactive molecules from temperature, moisture, and acidic conditions.

KEYWORDS: Alginate; chitosan; whey protein isolate; acylation; micronutrients; encapsulation; FTIR; SEM; stability; controlled release

INTRODUCTION

It is well-known that most micronutrients, including vitamins and minerals, are highly unstable in nature (*1*). They can be severely degraded during processing and storage depending on the environmental conditions such as relative humidity (RH) and temperature. In pharmaceutical formulations, degradations of vitamins and minerals were observed due to interactions of micronutrients in environmental conditions (*2*). Gastric acidity (pH < 2.0) can also induce loss of micronutrients in the stomach. Encapsulation is extensively used with success to enhance the stability of micronutrients and also permits a controlled release (*3*). A large variety of coating materials and methods have been developed to provide many advantages. A procedure to protect thiamin (a water-soluble vitamin) in bakery products was based on ethyl cellulose coating (*4*). However, it had the disadvantage of being more sensitive to moisture. Vitamin A (a fat-soluble vitamin) was encapsulated using a phase separation technique with a matrix made of cellulosic materials, fatty acids, proteins, and butylated hydroxytoluene (*5*). Although the efficiency of this method was demonstrated, the formulation involved the use of organic solvents and consequently limited its use for edible applications.

* Author to whom correspondence should be addressed [telephone (450) 687-5010; fax (450) 687-5792; e-mail monique.lacroix@iaf.inrs.ca].

With these difficulties, such as moisture sensitivity or organic solvent, in mind, several natural polymers have been studied for the development of a new encapsulation matrix. Alginate and chitosan are two naturally occurring polymers. Alginate is an anionic polysaccharide composed of mannuronic acid and guluronic acid residues, which is extracted from seaweed. Chitosan is a cationic polysaccharide obtained from partial deacetylation of chitin, the main constituent of the crustacean skeleton (*6*). These polymers are nontoxic, biodegradable, and biocompatible (*7*) and are also easily modified through physical or chemical methods (*8*). They are widely used in encapsulation applications due to their ability to form gels in the presence of certain divalent cations such as calcium, barium, and strontium (*9, 10*) by ionotropic gelation. Nevertheless, gel erosion is an important problem of alginate beads because it accelerates the release of the encapsulated substance (*11*). To suppress this phenomenon, a new formulation incorporating chitosan was elaborated (*12, 13*). In addition, acylation using fatty acid derivatives could even enhance the hydrophobic properties of the polymer (*8*). Consequently, the encapsulated substance could be protected against moisture and the controlled release mechanism was improved (*14*). Whey protein isolate (WPI, ≈90% protein) is a low-cost byproduct of cheese manufacturing, commonly used for its nutritional value and ability to form gels and emulsions (*15*). WPI was used in our study as an

10.1021/jf703739k CCC: $40.75
Published on Web 03/07/2008

encapsulation component to protect micronutrients against environmental conditions because beads containing WPI showed successful protection for immobilized bacteriocin (*16*).

An ideal encapsulation system for micronutrients is to reduce the reactivity of the micronutrient in relation to the outside environment: it would have a maximal stability in acidic pH and resist extreme moisture conditions. The aim of the present study was to develop a new encapsulation method for water-soluble vitamins, fat-soluble vitamins, and minerals. A matrix based on (i) native or acylated alginate and WPI (core) and (ii) native or acylated chitosan and WPI (external layer) was formulated. Polymer functionalization was characterized by Fourier transform infrared (FTIR) spectroscopy. Beads were formed by ionotropic gelation via calcium cross-linking and by alginate−chitosan complex coacervation, and the effect of the polymer modification on their microstructure was also examined. The rheological and mechanical properties of gels were investigated because they are of great importance for stability and controlled release studies. The stability of selected encapsulated micronutrients was also studied under different storage conditions of temperature and RH. Finally, the controlled release of encapsulated micronutrients was evaluated by simulating the gastrointestinal system.

MATERIALS AND METHODS

Materials. Sodium alginate (from brown algae, M_w 1.5 × 10^5 Da, low viscosity, 67% L-guluronic acid), ninhydrin reagent, D-glucosamine, and all micronutrients (ferrous fumarate, ascorbic acid, and β-carotene) were purchased from Sigma-Aldrich Canada Ltd. (Oakville, ON, Canada). Chitosan (Kitomer, M_w 1600 kDa, 85–89% deacetylation degree) was obtained from Marinard Biotech Inc. (Rivièreaux-Renards, QC, Canada). WPI (97.8% protein content, w/w) was from Davisco Foods International Inc. (Eden Prairie, MN). Palmitoyl chloride was from Fluka Biochemika (Buchs, Switzerland). The other reagents were purchased from Laboratoire MAT (Montreal, QC, Canada) and used without further purification.

Polymer Synthesis and Structural Analysis. *(a) Alginate O-Acylation and Chitosan N-Acylation.* Polymer modifications (O-acylation of alginate and N-acylation of chitosan) were prepared according to a method developed in our laboratory. An amount of 5 g of alginate was dissolved in 600 mL of distilled water, and the same amount of chitosan was dissolved in 600 mL of aqueous acetic acid (0.12 M, pH 4), respectively, at room temperature. The mixtures were stirred overnight to ensure a complete solubility. Thereafter, the pH of solutions was adjusted to 7.5 by the slow addition of 0.1 M NaOH, and the volumes were adjusted to about 800 mL. The acylation reactions were carried out by adding palmitoyl chloride (d = 0.907 g/mL) to polymer solutions in a ratio of 1:4 (w/w), maintaining the pH at 7.5 with 0.5 M NaOH, at 80 °C for alginate and at 55 °C for chitosan, respectively. After 1 h, the reaction media were neutralized (pH 6.8–7.0) and precipitated with acetone. The precipitate, collected by filtration, was washed at 50 °C with an excess of methanol and decanted. The washing was repeated twice to eliminate free fatty acids. Finally, the modified products were dried with pure acetone to obtain the corresponding functionalized polymer powders (O-acylated alginate and N-acylated chitosan) (*8*).

(b) Structural Analysis by FTIR Spectroscopy. FTIR spectra of acylated alginate and chitosan were recorded using a Spectrum One spectrophotometer (Perkin-Elmer, Woodbridge, ON, Canada) equipped with an attenuated total reflectance (ATR) device for solids analysis and a high-linearity lithium tantalate (HLLT) detector. Spectra were analyzed using Spectrum software (version 3.02.01). Native and functionalized polymers in powder form (20 mg) were placed onto a zinc selenide crystal, and the analysis was performed within the spectral region of 650–4000 cm^{-1} with 128 scans recorded at 4 cm^{-1} resolution. After attenuation of total reflectance and correction of the baseline, spectra were normalized with a limit ordinate of 1.5 absorbance units. Resulting FTIR spectra were compared to evaluate chemical modifications.

Preparation of Beads. *(a) Bead-Forming Solutions.* Two core bead solutions and two coating solutions were prepared. Core bead solutions contained 1.5% of WPI and 3% of native or functionalized alginate. Coating solutions (for external layer) contained 1.5% of WPI and 0.5% of native or functionalized chitosan.

(b) Bead Formation by Cross-Linking and Coacervation. Each core bead solution was dropped through an 18-gauge needle (38.1 mm length, 1.8 mm diameter) from a 60 mL plastic syringe into a beaker containing a calcium chloride solution (10%, w/v) under gentle stirring, at room temperature. The formed beads were allowed to harden for 30 min and then rinsed with distilled water. Thereafter, native and functionalized alginate beads were put into native and functionalized chitosan coating solutions, respectively, for 1 h under gentle stirring at room temperature. Beads were dried overnight at 20 °C and 40–50% RH. The average size of beads (2.6 ± 0.3 mm diameter) was measured with a Mitutoyo digimatic indicator (Mitutoyo MFG, Tokyo, Japan).

Characterization of Beads. *(a) Scanning Electron Microscopy (SEM) Analysis.* The three-dimensional surface and cross sectional structures of the beads were observed using a SEM (Hitachi S-4300SE/N, Hitachi Canada Ltd., Mississauga, ON, Canada). For the cross section observation, beads were cut using a sharp razor. Then, beads were deposited on a brass hold and sputtered with gold (150–180 Å coating thickness) in a Polaron PS3 sputter coater (Soquelec Ltd., Mississauga, ON, Canada). SEM photographs were taken with a magnification of 600× at room temperature. The working distance was maintained between 12 and 15 mm, and the acceleration voltage was 20 kV, with the electron beam directed to the surface at a 45° angle and a secondary electron imaging (SEI) detector.

(b) Rate of Gel Swelling. A water uptake apparatus was designed to study the water absorption properties of beads and consequently to determine the rate of gel swelling. Beads were dried at 40 °C for 24 h in a drying oven and placed in a 5 mL graduated cylinder (0.2 mL subdivision). Water penetration into beads was measured as a function of time. The water uptake was expressed in rate of gel swelling (percent volume increase).

(c) Water Vapor Permeability. Water vapor permeability (WVP) was measured from films made of the same solutions described above for bead preparation. Films were cast by applying 10 mL of core solutions onto Petri dishes (8.5 cm diameter; VWR Int., Ville Mont-Royal, QC, Canada) and allowed to dry overnight at room temperature and 40–50% RH. Dried water-soluble films were then peeled, immersed for 30 min in 10% (w/v) calcium chloride solution for cross-linking treatment, and then rinsed with distilled water. Thereafter, native and functionalized alginate films were put into native and functionalized chitosan coating solution, respectively, for 1 h, allowing polyanion−polycation complex coacervation, and dried overnight at room temperature and 40–50% RH. WVP tests were conducted gravimetrically using an ASTM procedure (*17*). The films were mechanically sealed onto Vapometer cells (No. 68-1, Kalamazoo Paper Chemicals, Richland, WA) containing 30 g of anhydrous calcium chloride. The cells were initially weighed and placed in a Shellab 9010L controlled humidity chamber (Sheldon Manufacturing Inc., Cornelius, OR) at 30 °C and 100% RH for 24 h. WVP was calculated according to the formula

$$\text{WVP}\ (\text{g}\cdot\text{mm/m}^2\cdot 24\ \text{h}\cdot\text{mmHg}) = W\cdot x/A\cdot T(P_2 - P_1) \quad (1)$$

where W is the weight gain of the cell (g) after 24 h, x is the film thickness (mm), A is the area of exposed film (31.67 × 10^{-4} m^2), and ($P_2 - P_1$) is the differential vapor pressure across the film ($P_2 - P_1$ = 17.82 mmHg at 30 °C). Film thickness was measured using a Mitutoyo digimatic indicator at five random positions around the film, by slowly reducing the micrometer gap until the first indication of contact.

(d) Puncture Tests. Puncture strength (PS) and puncture deformation (PD) measurements were carried out using a Stevens-LFRA texture analyzer (model TA-1000; Texture Technologies Corp., Scarsdale, NY), as described by Salmieri and Lacroix (*18*). The same film samples used for WVP measurements were equilibrated in a desiccator containing a saturated sodium bromide solution ensuring 56% RH at room temperature (21 °C) for at least 24 h. Films were then fixed between two perforated plexiglass plates (3.2 cm diameter), and the holder was held tightly with two screws. A cylindrical probe (2 mm diameter) was

moved perpendicularly to the film surface at a constant speed (1 $mm \cdot s^{-1}$) until it passed through the film. Strength and deformation values at the puncture point were used to calculate the hardness and deformation capacity of the film. To avoid any variation related to the film thickness, the PS values were divided by the thickness of the films. PS was calculated using the equation

$$PS\ (N \cdot mm^{-1}) = (9.81 \times F)/x \quad (2)$$

where F is the recorded force value (g), x is the film thickness (μm), and 9.81 $m \cdot s^{-2}$ is the gravitational acceleration.

PD was calculated from the PS curve, using the equation

$$PD\ (mm) = d/8.33 \quad (3)$$

where d is the distance (mm) recorded between the time of first contact probe/film and the time of puncture point and 8.33 is a corrective factor related to the fixed parameters of the texture analyzer.

(e) Viscoelasticity. Viscoelastic properties were evaluated using relaxation curves. The same procedure for puncture tests as described before was used, but the probe was stopped at 3 mm and maintained for 1 min. The viscoelastic coefficient (Y) was calculated using the equation

$$Y_{1min} = (F_i - F_f)/F_i \quad (4)$$

where F_i is the initial recorded value (g) and F_f the second value measured after 1 min of relaxation.

Stability Studies. *(a) Experimental Design.* A simple factorial design with two factors was performed to determine the stability of encapsulated and nonencapsulated micronutrients in normal (23 °C, 56% RH) and extreme (45 °C, 100% RH) conditions. The RH of 56% was obtained using a desiccator containing saturated sodium bromide solution, and it was placed in an incubator to control temperature (23 °C). The RH of 100% at 45 °C was obtained using a controlled humidity chamber (Shellab 9010L; Sheldon Manufacturing Inc.). The overall experimental design was performed in two replications. Samples were stored for up to 6 months and were taken periodically for analysis of vitamins and mineral. For each parameter, tests were performed in triplicate.

(b) Sample Preparation. Ascorbic acid (1.5%, w/v; water-soluble vitamin), ferrous fumarate (1.5%, w/v; mineral), and β-carotene (0.5%, w/v; fat-soluble vitamin) were added individually in each core bead solution before ionic gelation with calcium and chitosan, as described above. Bead samples consisting of 100 mg of encapsulated ascorbic acid, ferrous fumarate, or β-carotene were placed in hermetic plastic bags and stored in appropriate desiccators. The same amounts of each micronutrient without bead-forming polymers were also prepared as nonencapsulated samples and placed in the same conditions with encapsulated bead samples.

(c) Determination of Micronutrient Concentration. Prior to the determination of micronutrient concentration, beads were dissolved in phosphate buffer (KH_2PO_4, 0.1 M, pH 8) under gentle stirring at room temperature. Ascorbic acid was extracted using a Sep-Pak Plus C-18 cartridge (Waters Co., Milford, MA) according to the method of Lavigne et al. (*19*). Separation and quantification of ascorbic acid were performed using a HPLC system (model Vista 5500, Varian Co., Walnut Creek, CA) equipped with an LC-8-DB column (Sigma-Aldrich Canada Ltd.). A solution of methanol/hexane sulfonate (4.3 mM) (15:85, v/v) was used as a mobile phase. Detection was performed using a UV detector (model 2550, Varian Co.). Identification of ascorbic acid was based on its retention time. Thiamin (vitamin B_1) was used as an internal standard and allowed to determine the yield of extraction recovery. β-Carotene was extracted using hexane following the method of Epler et al. (*20*). Separation and quantification were performed using a HPLC system, equipped with an LC-18 column (Sigma-Aldrich Canada Ltd.). A solution of methanol/Milli-Q water 95:5 (v/v) was used as a mobile phase. Identification of β-carotene was based on its retention time. Ergocalciferol (vitamin D_2) was used as an internal standard and allowed to determine the yield of extraction recovery. Ferrous fumarate concentration was determined using a SpectrAA 10 series atomic absorption spectrometer (Varian Co.).

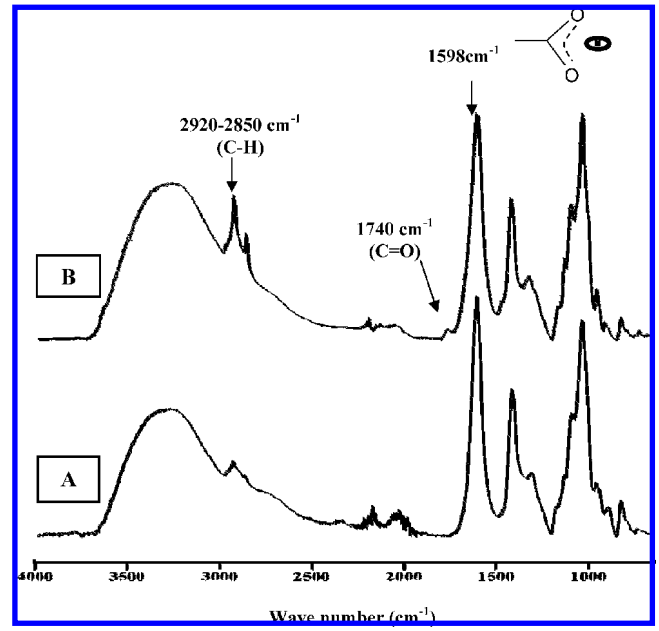

Figure 1. FTIR spectra of (**A**) native (nonfunctionalized) and (**B**) functionalized alginate.

Release Studies in Gastrointestinal Media. *(a) Sample Preparation.* Samples were composed of 1 g of beads containing ascorbic acid, β-carotene, or ferrous fumarate as the micronutrient. Beads were prepared and dried as described above.

(b) Controlled Release of Micronutrients. The release study of micronutrient was performed under gastric and intestinal simulating treatments. The gastric and intestinal solutions were formulated according to the United States Pharmacopeia (*21*). Gastric solution was composed of 3.2 g/L of pepsin and 2.0 g/L of NaCl, and the final pH was adjusted to 1.5 by the addition of HCl (1.0 M). Intestinal solution consisted of 6.8 g/L of sodium phosphate buffer and 10 g/L of pancreatin, and the pH was adjusted to 7.5 ± 0.1 using NaOH (0.2 N). One gram of beads was added to 30 mL of gastric solution under gentle stirring for 30 min, at 37 °C. The solution was withdrawn (1 mL), and the micronutrient concentration was determined as described above for stability studies. Then, beads were transferred from a gastric solution to an intestinal solution and stirred gently for 6 h at 37 °C (*22*). A volume of 1 mL of this solution was withdrawn periodically, and the micronutrient concentration was determined as described above for stability studies.

Statistical Analysis. The experiment for the evaluation of gel swelling was carried out using a 3 × 3 × 2 × 14 factorial design (3 replicates, 3 samples/replicate, 2 types of gels, 14 times of measurement). Experiments for the determination of WVP and mechanical properties of gels were carried out using a 3 × 10 × 2 factorial design (3 replicates, 10 samples/replicate, 2 types of gels). Stability studies were performed using a 2 × 3 × 3 × 2 × 3 × 8 factorial design (2 replicates, 3 samples/replicate, 3 bead treatments, 2 ambient conditions, 3 micronutrients, 8 times of measurement). Controlled release studies were performed using a 3 × 3 × 2 × 3 × 12 factorial design (2 replicates, 3 samples/replicate, 2 bead treatments, 3 micronutrients, 12 times of measurement). Data analyses were carried out using SPSS Base 10.0 software (Stat-Packets statistical analysis software, SPSS Inc., Chicago, IL). Differences between means for two groups were determined using analysis of variance and the Student t test. Differences between more than two groups were determined using analysis of variance and Duncan's multiple-range tests. Differences between means were considered to be significant when $p \leq 0.05$.

RESULTS AND DISCUSSION

Acylation of Polymers. Figure 1 shows the FTIR spectra of native (**A**) and functionalized (**B**) alginate. For native alginate, the absorption band at 1598 cm^{-1} can be assigned to asymmetric

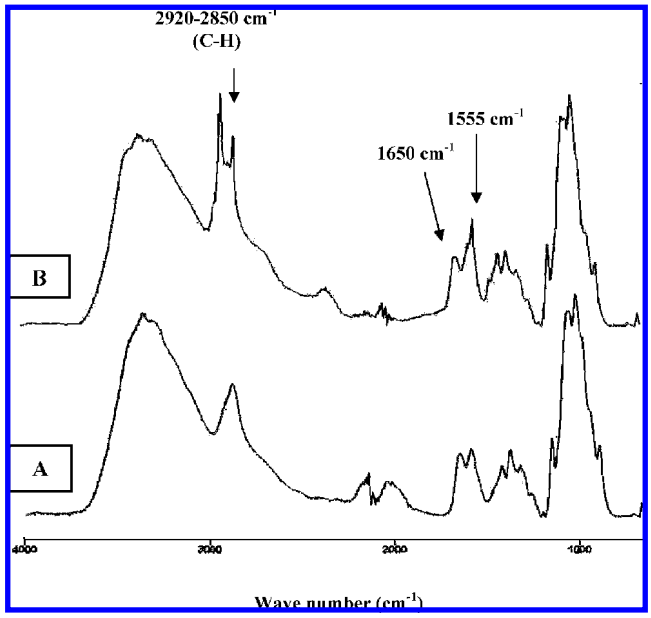

Figure 2. FTIR spectra of (**A**) native (nonfunctionalized) and (**B**) functionalized chitosan.

and symmetric COO^- stretching vibration. After O-acylation, a new band at 1740 cm^{-1} due to carbonyl stretching vibration of the *O*-acyl group (ester linkage) was noted. In addition, peaks at 2920–2850 cm^{-1} were ascribed to overlapping symmetric and asymmetric C−H stretching vibration of aliphatic chains ($-CH_2-$, $-CH_3$), and their intensity also increased after O-acylation. As reported by Le Tien et al. (*23*) and Franklin et al. (*24*), these results clearly confirmed that alginate was O-acylated by indicating the presence of aliphatic chains substituted on alginate via −CO−O− links.

Figure 2 shows the FTIR spectra of native (**A**) and functionalized (**B**) chitosan. The absorption peak at 1650 cm^{-1} can be assigned to the C═O stretching vibration of secondary amides (amide I band), and the peak at 1555 cm^{-1} is associated with N−H bending and C−N stretching vibrations of amides (amide II band) (*22*). After N-acylation, an increase of these two vibrational bands was observed, indicating an increase of 2-amido-glucose units. In addition, as described for alginate acylation, the intensity of peaks at 2920–2850 cm^{-1} ascribed to palmitoyl chains also increased after N-acylation. As reported by Le Tien et al. (*8*), these results clearly confirmed that chitosan was N-acylated by indicating the presence of aliphatic chains substituted on chitosan via amide links.

Characterization of Beads. *(a) SEM Analysis.* SEM microstructures of surface and cross section of encapsulated beads are presented in **Figure 3**. Results depict the images of native (**A**) and functionalized (**B**) alginate−chitosan beads. Both beads were characterized by a core alginate and an external chitosan layer. Surface images showed that functionalized beads had a smoother outer surface. In contrast, native beads showed rough, granular, and undulating surfaces. It was obvious that the surface smoothness in functionalized beads was apparently affected by acylation modification in chitosan layer. Thus, functionalization of polymer affected the surface smoothness of the beads.

Microstructures of cross section showed a difference in thickness of the external layer of native and functionalized beads. Native beads had a thinner outer layer. On the other hand, functionalized beads had a thicker outer layer, which was caused by acylation modification. Added palmitoyl chains increased hydrophobic interactions in chitosan and alginate layers. Acylation modification obviously makes a steric hindrance to the

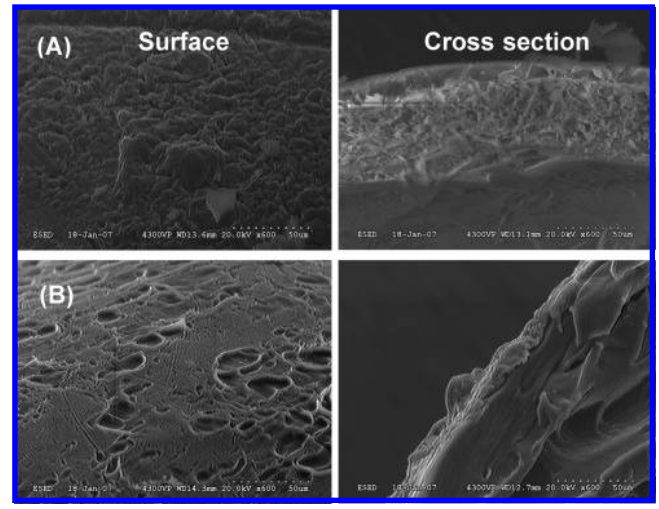

Figure 3. SEM micrographs of the surface (left) and cross section (right) of (**A**) native and (**B**) functionalized alginate−chitosan beads. Bead surface and cross section were viewed at a magnification of 600×.

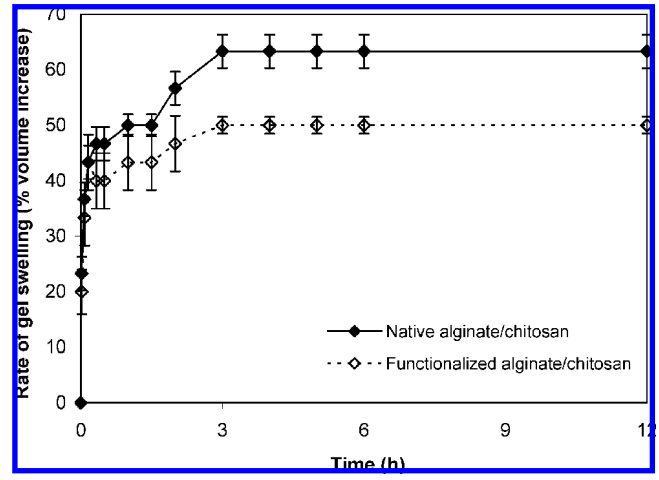

Figure 4. Rate of gel swelling (percent volume increase) of native and functionalized beads.

cross-links between calcium ions and carboxylate groups of alginate and increases hydrophobic interaction in core bead, implying a dense and homogeneous structure. The functionalized polymers appeared to be more compact in comparison with the native polymers. The native polymers were essentially characterized by ionic interactions and hydrogen associations between chitosan and alginate layers, whereas functionalized polymers presented more hydrophobic interactions as well as ionic interactions between functionalized chitosan and alginate layers (*8*).

The thickness of the external layer was homogeneous surrounding the core layer, regardless of native or functionalized polymers. These observations indicate that encapsulation makes a good protection of inner micronutrients against degradation.

(b) Gel Swelling. Water absorption behavior of beads as a function of time is presented in **Figure 4**. Results showed that the rate of gel swelling was influenced by the functionalization of polymers (alginate and chitosan). Functionalized polymers allowed a significant ($p \leq 0.05$) decrease of water absorption by beads when compared to native polymers after 1 h and up to the end of the experiment. This barrier effect may be caused by the hydrophobic interactions induced in functionalized alginate and functionalized chitosan. The water uptake is an

Table 1. Water Vapor Permeability of Native and Functionalized Films

nature of film	WVP[a] (g·mm/m^2·24 h·mmHg)
native alginate−chitosan	25.18 ± 1.85 a
functionalized alginate−chitosan	21.13 ± 1.63 b

[a] Means that are not followed by a common letter are significantly different ($p \leq 0.05$) between native (nonfunctionalized) and functionalized films.

Table 2. Mechanical Properties of Native and Functionalized Films

nature of film	puncture strength[a] (N/mm)	puncture deformation[a] (mm)	viscoelastic coefficient[a]
native alginate−chitosan	205.8 ± 15.6 a	1.64 ± 0.01 a	0.78 ± 0.03 a
functionalized alginate−chitosan	206.2 ± 20.0 a	1.59 ± 0.02 b	0.85 ± 0.03 b

[a] Means that are not followed by a common letter are significantly different ($p \leq 0.05$) between native (nonfunctionalized) and functionalized beads.

important factor closely related to the controlled release of encapsulated micronutrients. In fact, important water absorption leads to the dissolution of the beads and faster release of encapsulated micronutrients.

(c) Water Vapor Permeability (WVP). WVP of gels is presented in **Table 1**. Results showed that functionalization significantly ($p \leq 0.05$) improved the water barrier property of film. The WVP value of functionalized gels was 21.13 g·mm/m^2·24 h·mmHg, whereas that of native gels was 25.18 g·mm/m^2·24 h·mmHg. This observation confirmed that hydrophobic and polyionic interactions between functionalized alginate and functionalized chitosan increased hydrophobicity and then decreased the WVP (*8*).

(d) Puncture Strength (PS) and Puncture Deformation (PD). The PS and PD of gels are presented in **Table 2**. Results showed that the PS of gels was not affected by functionalization. The puncture value of native gels (205.8 N/mm) was not significantly ($p > 0.05$) different from that of functionalized gels (206.2 N/mm). On the other hand, the PD of gels decreased significantly ($p \leq 0.05$) by functionalization. Indeed, the deformation value of native gels was 1.64 mm, whereas that of functionalized gels was 1.59 mm. As previously described, this result could be explained by the presence of fatty acids in the polymer matrix, increasing hydrophobic interactions that probably interfere with ionic and polymer–polymer interactions. Similar observations were reported by Salmieri and Lacroix (*18*) and Le Tien et al. (*15*).

(e) Viscoelasticity. Viscoelastic properties of gels are presented in **Table 2**. A low viscoelastic coefficient (*Y*) means that the material is highly elastic, whereas a high coefficient indicates that the material is more rigid and easily distorted. Functionalization resulted in a significant ($p \leq 0.05$) effect on beads' viscoelasticity. A *Y* coefficient of 0.78 was observed for native gels, as compared to 0.85 for functionalized gels. Indeed, formation of hydrophobic interactions by functionalization decreased the elasticity of the gels, probably due to similar hydrophobic interferences that affected the PD. Similar behaviors were reported by Ressouany et al. (*25*) and Sabato et al. (*26*). Their studies showed a loss of gel elasticity after the addition of more hydrophobic components in their film formulations.

Stability Studies. *(a) Ferrous Fumarate.* **Figure 5** presents the effect of encapsulation on the retention rate of ferrous fumarate under normal (**A**; 23 °C, 56% RH) and extreme (**B**; 45 °C, 100% RH) conditions of storage. Results showed an important decrease of nonencapsulated ferrous fumarate in comparison with encapsulated ferrous fumarate after 6 months of storage, notwithstanding the conditions of temperature and RH (**Figure 5**). From day 1 to day 180, under normal conditions (**Figure 5A**), the degradation rate of nonencapsulated ferrous fumarate was 49.39%, as compared to 19.15 and 18.09% for ferrous fumarate encapsulated in beads consisting of native and functionalized polymers, respectively. These observations were prominent under extreme conditions (**Figure 5B**). Indeed, at day 180, the degradation rate of nonencapsulated ferrous fumarate was 74.54%. However, encapsulation remained efficient in extreme storage conditions, with degradation values of 18.27% for native beads and 21.62% for functionalized beads. It is also interesting to note an important difference in the slopes from day 0 to day 60, between nonencapsulated and encapsulated ferrous fumarate, indicating an optimal efficiency of encapsulation in this period of storage. Hence, these results demonstrated the efficiency of encapsulation for ferrous fumarate retention, although no difference was observed between the encapsulations by native and functionalized polymers.

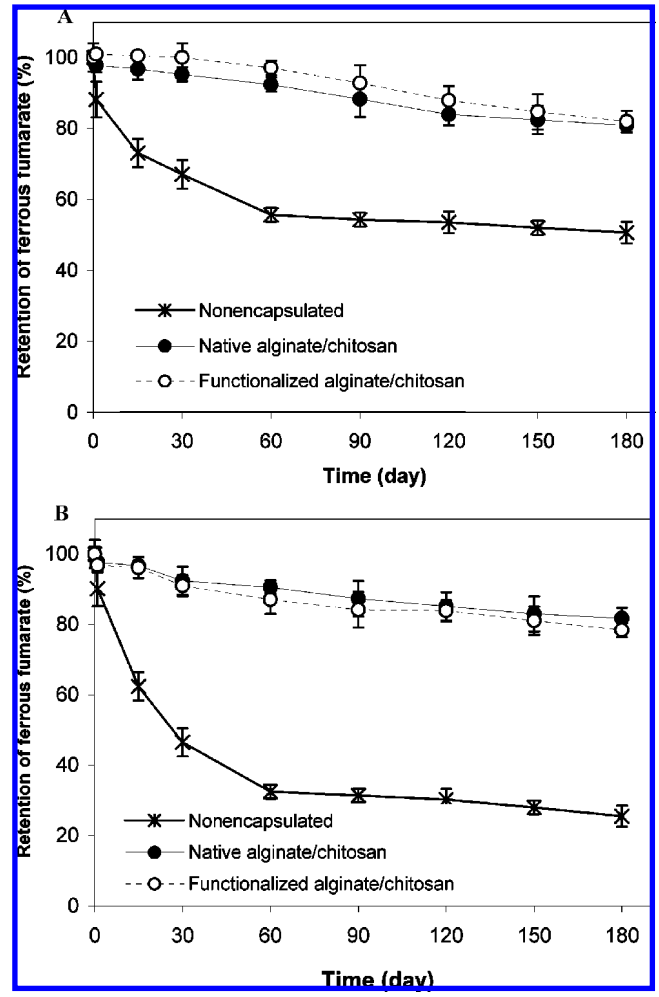

Figure 5. Ferrous fumarate stability under two storage conditions: (**A**) 23 °C and 56% RH; and (**B**) 45 °C and 100% RH.

(b) Ascorbic Acid. **Figure 6** presents the effect of encapsulation on the retention rate of ascorbic acid under normal (**A**) and extreme (**B**) conditions of storage. Results show an important decrease of nonencapsulated ascorbic acid in comparison with encapsulated acid after 6 months of storage only for extreme conditions (**Figure 6B**). From day 1 to day 180, the degradation rate of nonencapsulated ascorbic acid was 72.15%, as compared to 20.42 and 16.34% for ascorbic acid

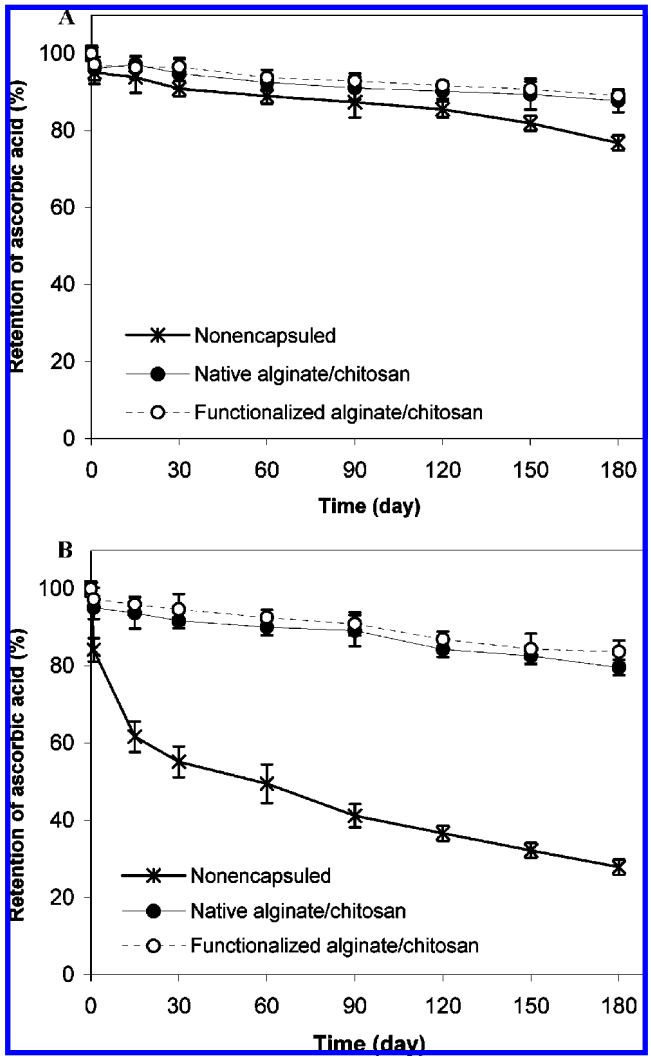

Figure 6. Ascorbic acid stability under two storage conditions: (**A**) 23 °C and 56% RH; (**B**) 45 °C and 100% RH.

encapsulated in beads consisting of native and functionalized polymers, respectively. These observations were more prominent under extreme conditions (**Figure 6B**) than under normal conditions (**Figure 6A**), where nonencapsulated ascorbic acid was not much degraded as compared to encapsulated ascorbic acid, with approximately similar degradation values after 180 days of storage. It is also interesting to note an important difference in the slopes from day 0 to day 15 in extreme conditions (**Figure 6B**) between nonencapsulated and encapsulated ascorbic acid, indicating an optimal efficiency of encapsulation in this period of storage. Hence, these results demonstrated the efficiency of encapsulation for ascorbic acid retention, although no difference was observed between the encapsulations by native and functionalized polymers.

(b) β-Carotene. **Figure 7** presents the effect of encapsulation on the retention rate of β-carotene under normal (**A**) and extreme (**B**) conditions of storage. As for ascorbic acid observations, results showed an important decrease of nonencapsulated β-carotene in comparison with encapsulated β-carotene after 6 months of storage only for extreme conditions (**Figure 7B**). From day 1 to day 180, the degradation rate of nonencapsulated β-carotene was 75.29%, as compared to 12.28 and 11.71% for β-carotene encapsulated in beads consisting of native and functionalized polymers, respectively. These observations were more prominent under extreme conditions (**Figure 7B**) than normal conditions (**Figure 7A**), where nonencapsulated β-carotene is not much degraded as compared to encapsulated β-carotene, with approximately the same range of degradation values after 180 days of storage. It is also interesting to note an important difference in the slopes from day 0 to day 90 in extreme conditions (**Figure 7B**) between nonencapsulated and encapsulated β-carotene, indicating an optimal efficiency of encapsulation in this period of storage. As for ascorbic acid retention, these results demonstrated the efficiency of encapsulation for β-carotene retention, although no difference was observed between the encapsulations by native and functionalized polymers.

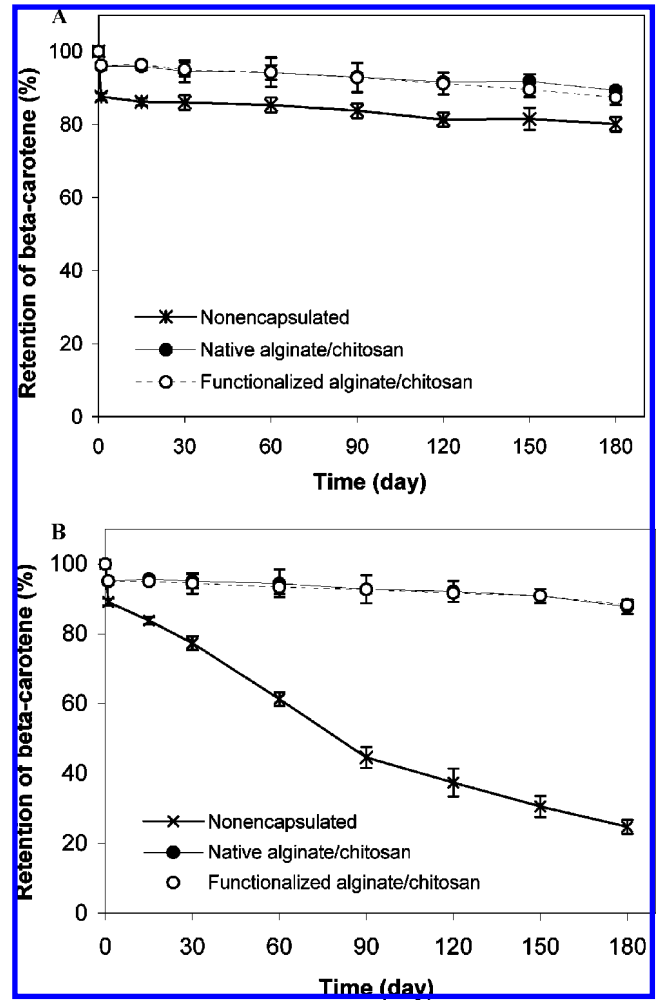

Figure 7. β-Carotene stability under two storage conditions: (**A**) 23 °C and 56% RH; (**B**) 45 °C and 100% RH.

These results suggest that encapsulation is efficient followed by the nature of encapsulated micronutrient and storage conditions. Nonencapsulated ferrous fumarate was not as stable as nonencapsulated ascorbic acid and β-carotene in normal conditions, implying an important degradation rate as compared to encapsulated fumarate (**Figure 5A**). In extreme conditions, encapsulation was significantly efficient for all micronutrients during the storage. In addition, optimal periods of storage varied with encapsulated nutrients in extreme conditions, with 15 days for ascorbic acid, 60 days for ferrous fumarate, and 90 days for β-carotene, confirming the different degrees of sensitivity of the micronutrients to the environmental conditions (*1*).

Release Studies in Gastrointestinal Media. The release profiles of encapsulated ferrous fumarate, ascorbic acid, and β-carotene in gastrointestinal media, simulating a pepsin at pH 2 followed by a pancreatin at pH 7.5, are presented in **Figure 8**. Results showed the same pattern of release profile, but

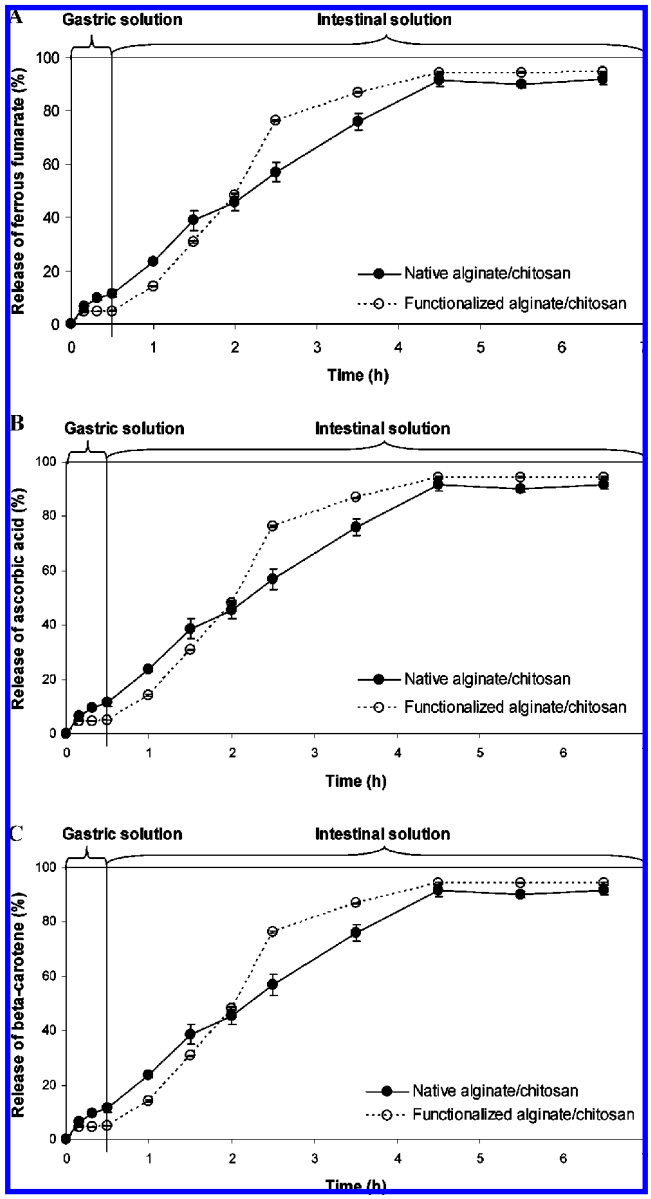

Figure 8. Controlled release of (**A**) ferrous fumarate, (**B**) ascorbic acid, and (**C**) β-carotene under gastrointestinal conditions.

different micronutrients were encapsulated nevertheless. This release behavior can be characterized in three steps. First, in the presence of pepsin at pH 2, a slight release of micronutrients into the gastric media was recorded. This good resistance of encapsulated beads during the transit in stomach condition can be explained not only by the existence of an external layer of chitosan−alginate coacervate surrounding core beads but also by the fact that alginate is insoluble at this pH. Moreover, the release rate from functionalized beads is slower than that from native beads, probably due to the presence of fatty acids that improves matrix cohesion by hydrophobic interactions, decreases water absorption, and consequently delays the diffusion by swelling. Second, micronutrients were released rapidly into the intestinal media with the same release tendency between 30 min and 4 h. Furthermore, it was interesting to note a typical profile in this second step because an inflection point appeared after 2 h. Indeed, results indicated that release was slower for functionalized beads than native beads between 30 min and 2 h, whereas it turned to be faster for functionalized beads after 2 h until 4 h. To explain this release behavior, it could be hypothesized that (i) minimal water absorption of functionalized polymers favors swelling in such conditions that hydrophobic interactions cannot maintain cohesive forces within polymeric matrix and (ii) the presence of fatty acids in functionalized polymers favors the degradation of matrix due to heterogeneous structure, suggesting stability of polymer structure by functionalization from 30 min to 2 h. Third, approximately 90% of micronutrients were released from native and functionalized beads after 4 h, and this percentage of released micronutrients was at equilibrium up to 6.5 h. These results showed that encapsulation efficiently controlled release of micronutrients until 4 h, reaching the maximum release percentage, but functionalization did not affect the release rate after 4 h. In this context, release study demonstrated that micronutrients were protected from enzymatic and acidic environments by encapsulation, showing a controlled release mechanism of micronutrients during the gastrointestinal transit (*8*).

In summary, this study allowed the development of a new encapsulation method involving two polymers (alginate and chitosan) and using methods of functionalization (acylation) and gelation/coacervation to improve the stability and physicochemical properties of beads. The main difference between native and functionalized beads consisted in the presence of fatty acid chains in the core (palmitoylated alginate) and external layer (palmitoylated chitosan) of beads. Hence, alginate cross-links improved insolubility of beads by ionotropic gelation and alginate−chitosan coacervation, which led to polyionic links between the core bead and the external layer. Functionalization increased hydrophobic interactions into polymeric matrix, involving structural changes that were characterized by FTIR and SEM analyses. In addition, functionalization improved the polymers' barrier property by decreasing water uptake and WVP. Functionalized polymers did not improve their mechanical properties at break, decreasing PD and viscolelasticity. Although no difference was observed in the stability of micronutrients encapsulated in native and functionalized beads, encapsulation strongly increased the stability of ferrous fumarate, ascorbic acid, and β-carotene under extreme (45 °C, 100% RH) storage conditions. A release study in gastrointestinal media revealed that encapsulated beads were not susceptible to enzymatic and acidic attacks during transit in the stomach. This study also demonstrated that encapsulation had an excellent capacity to protect bioactive molecules against temperature, humidity, and acidic conditions and allowed a controlled release of these compounds during gastrointestinal transit. Therefore, the potential use of this new encapsulation method could be further explored and could be of great interest for cosmetic, pharmaceutical, and food uses.

ACKNOWLEDGMENT

We thank M. Raymond Mineau (Département des Sciences de la Terre et de l'Atmosphère, UQÀM) for his technical assistance with SEM photographs.

LITERATURE CITED

(1) Harris, R. S. General discussion on the stability of nutrients. In *Nutritional Evaluation of Food Processing*, 3rd ed.; Karmas, E., Harris, R. S., Eds.; Van Nostrand Reinhold: New York, 1988.
(2) Sandström, B. Micronutrient interactions: effects on absorption and bioavailability. *Br. J. Nutr.* **2001**, *85*, S181–S185.
(3) Shahidi, F.; Han, X.-Q. Encapsulation of food ingredients. *Crit. Rev. Food Sci. Nutr.* **1993**, *33*, 501–547.
(4) Morse, L. D.; Hammes, P. A.; Boyd, W. A. Devil's food cake and other alkaline bakery goods. U.S. Patent 3,821,422, 1974.
(5) Markus, A.; Pelah, Z. Encapsulation of vitamin A. *J. Microencapsul.* **1989**, *6*, 389–394.

(6) Rinaudo, M.; Domard, A. Solution properties of chitosan. In *Chitin and Chitosan*; Skjak-Braek, G., Anthonsen, T., Sandford, P., Eds.; Elsevier: New York, 1989; pp 71–83.
(7) Shapiro, L.; Cohen, S. Novel alginate sponges for cell culture and transplantation. *Biomaterials* **1997**, *18*, 583–590.
(8) Le Tien, C.; Lacroix, M.; Ispas-Szabo, P.; Mateescu, M.-A. *N*-acylated chitosan: hydrophobic matrices for controlled drug release. *J. Controlled Release* **2003**, *93*, 1–13.
(9) Ramadas, M.; Paul, W.; Dileep, K. J.; Anitha, Y.; Sharma, C. P. Lipoinsulin encapsulated alginate−chitosan capsules: intestinal delivery in diabetic rats. *J. Microencapsul.* **2000**, *17*, 405–411.
(10) Braccini, I.; Perez, I. Molecular basis of Ca^{++}-induced gelation in alginate and pectin: the egg-box model revisited. *Biomacromolecules* **2001**, *2*, 1089–1096.
(11) Murata, Y.; Nakada, K.; Miyamoto, E.; Kawashima, S.; Seo, S. H. Influence of erosion of calcium-induced alginate gel matrix on the release of brilliant blue. *J. Controlled Release* **1993**, *23*, 21–26.
(12) Murata, Y.; Maeda, T.; Miyamoto, E.; Kawashima, S. Preparation of chitosan-reinforced alginate gel beads: effects of chitosan on gel matrix erosion. *Int. J. Pharm.* **1993**, *96*, 139–145.
(13) Polk, A.; Amsden, B.; Yao, K. D.; Peng, T.; Goosen, M. F. Controlled release of albumin from chitosan-alginate microcapsules. *J. Pharm. Sci.* **1994**, *83*, 178–185.
(14) Millette, M.; Le Tien, C.; Lacroix, M.; Mateescu, M. A.; Archambault, D.; Lamontagne, L.; Savard, R. *Protection de Bactéries Probiotiques par Immobilisation Dans des Biomolécules Marines*; presented at the Conférence sur les Biomolécules Marines de Rimouski, Québec, Canada, 2002.
(15) Le Tien, C.; Letendre, M.; Ispas-Szabo, P.; Mateescu, M.-A.; Delmas-Patterson, G.; Yu, H.-L.; Lacroix, M. Development of biodegradable films from whey proteins by cross-linking and entrapment in cellulose. *J. Agric. Food Chem.* **2000**, *48*, 5566–5575.
(16) Millette, M.; Le Tien, C.; Smoragiewicz, W.; Lacroix, M. Inhibition of *Staphylococcus aureus* on beef by nisin-containing modified alginate films and beads. *Food Control* **2007**, *18*, 878–884.
(17) Letendre, M.; D'Aprano, G.; Lacroix, M.; Salmieri, S.; St-Gelais, D. Physicochemical properties and bacterial resistance of biodegradable milk protein films containing agar and pectin. *J. Agric. Food Chem.* **2002**, *50*, 6017–6022.
(18) Salmieri, S.; Lacroix, M. Physicochemical properties of alginate/polycaprolactone-based films containing essential oils. *J. Agric. Food Chem.* **2006**, *54*, 10205–10214.
(19) Lavigne, C.; Zee, J. A.; Simard, R. E.; Gosselin, C. High-performance liquid chromatographic−diode-array determination of ascorbic acid, thiamine and riboflavin in goats' milk. *J. Chromatogr.* **1987**, *410*, 201–205.
(20) Epler, K. S.; Ziegler, E. G.; Craft, N. E. Liquid chromatographic method for the determination of carotenoids, retinoids and tocopherols in human serum and in food. *J. Chromatogr.* **1993**, *619*, 37–48.
(21) Simulated gastric fluid and simulated intestinal fluid, TS. In *The United States Pharmacopeia 23, The National Formulary 18*; The United States Pharmacopeial Convention, Inc.: Rockville, MD, 1995; pp 2053.
(22) Xu, J.; McCarthy, S. P.; Gross, R. A. Chitosan film acylation and effects on biodegradability. *Macromolecules* **1996**, *29*, 3436–3440.
(23) Le Tien, C.; Millette, M.; Mateescu, M.-A.; Lacroix, M. Modified alginate and chitosan for lactic acid bacteria immobilization. *Biotechnol. Appl. Biochem.* **2004**, *39*, 1–9.
(24) Franklin, M. J.; Douthit, S. A.; McClure, M. A. Evidence that the *algI/algJ* gene cassette, required for O-acetylation of *Pseudomonas aeruginosa* alginate, evolved by lateral gene transfer. *J. Bacteriol.* **2004**, *186* (14), 4759–4773.
(25) Ressouany, M.; Vachon, C.; Lacroix, M. Irradiation dose and calcium effect on the mechanical properties of cross-linked caseinate films. *J. Agric. Food Chem.* **1998**, *46*, 1618–1623.
(26) Sabato, S. F.; Ouattara, B.; Yu, H.; D'Aprano, G.; Le Tien, C.; Mateescu, M.-A.; Lacroix, M. Mechanical and barrier properties of cross-linked soy and whey protein-based films. *J. Agric. Food Chem.* **2001**, *49*, 1397–1403.

Received for review December 21, 2007. Revised manuscript received January 25, 2008. Accepted January 28, 2008.

JF703739K